The FASEB Journal article fj.14-257808. Published online January 28, 2015.



# The stretch responsive microRNA miR-148a-3p is a novel repressor of *IKBKB*, NF-κB signaling, and inflammatory gene expression in human aortic valve cells

**Vishal Patel,*[,1] Katrina Carrion,*[,1] Andrew Hollands,[†] Andrew Hinton,[‡] Thomas Gallegos,[§] Jeffrey Dyo,* Roman Sasik,[¶] Emma Leire,[†] Gary Hardiman,[‖,#] Salah A. Mohamed,** Sanjay Nigam,[§] Charles C. King,[‡] Victor Nizet,[†] and Vishal Nigam*[,††,2]**

*Department of Pediatrics (Cardiology), [†]Department of Pediatrics and School of Pharmacy, [‡]Pediatrics Diabetes Research Center, [§]Departments of Pediatrics and Cellular and Molecular Medicine, and [¶]Department of Medicine, University of California, San Diego, La Jolla, California, USA; [‖]Computational Science Research Center and Biomedical Informatics Research Center, San Diego State University, San Diego, California, USA; [#]Department of Medicine, Medical University of South Carolina, Charleston, South Carolina, USA; **Department of Cardiac Surgery, University Clinic of Schleswig-Holstein, Campus Luebeck, Luebeck, Germany; and [††]Rady Children's Hospital, San Diego, California, USA

ABSTRACT **Bicuspid aortic valves calcify at a significantly higher rate than normal aortic valves, a process that involves increased inflammation. Because we have previously found that bicuspid aortic valve experience greater stretch, we investigated the potential connection between stretch and inflammation in human aortic valve interstitial cells (AVICs). Microarray, quantitative PCR (qPCR), and protein assays performed on AVICs exposed to cyclic stretch showed that stretch was sufficient to increase expression of interleukin and metalloproteinase family members by more than 1.5-fold. Conditioned media from stretched AVICs was sufficient to activate leukocytes. microRNA sequencing and qPCR experiments demonstrated that miR-148a-3p was repressed in both stretched AVICs (43% repression) and, as a clinical correlate, human bicuspid aortic valves (63% reduction). miR-148a-3p was found to be a novel repressor of *IKBKB* based on data from qPCR, luciferase, and Western blot experiments. Furthermore, increasing miR-148a-3p levels in AVICs was sufficient to decrease NF-κB (nuclear factor kappa-light-chain-enhancer of activated B cells) signaling and NF-κB target gene expression. Our data demonstrate that stretch-mediated activation of inflammatory pathways is at least partly the result of stretch-repression of miR-148a-3p and a consequent failure to repress *IKBKB*. To our knowledge, we are the first to report that cyclic stretch of human AVICs activates inflammatory genes in a tissue-autonomous manner *via* a microRNA that regulates a central inflammatory pathway.—Patel, V., Carrion, K., Hollands, A., Hinton, A., Gallegos, T., Dyo, J., Sasik, R., Leire, E., Hardiman, G., Mohamed, S. A., Nigam, S., King, C. C., Nizet, V., Nigam V. The stretch responsive microRNA miR-148a-3p is a novel repressor of *IKBKB*, NF-κB signaling, and inflammatory gene expression in human aortic valve cells. *FASEB J.* 29, 000–000 (2015). www.fasebj.org**

*Key Words: inflammation · NF-κB · aortic valve calcification · mechanotransduction*

STRETCH IS A MAJOR BIOMECHANICAL stimulus; a wide variety of cells in the body—such as cardiac, vascular, skeletal, skin, muscle, and gastrointestinal cells—are exposed to stretch. In particular, the response of cells in the heart and blood vessels to stretch is important because they are exposed to stretch every time the heart beats. Although stretch has been shown to activate NF-κB (nuclear factor kappa-light-chain-enhancer of activated B cells) signaling (1, 2), the mechanism is not understood. MicroRNAs (miRNAs) are small noncoding RNAs (20 to 24 base pairs long) that play important regulatory roles by binding to target mRNAs to promote degradation or block translation of their target mRNAs. One mechanism by which miRNAs can repress NF-κB signaling is by targeting *IKBKB*, which encodes IκB kinase β (IKKβ) (3–5). IKKβ phosphorylates IκB, resulting in dissociation of IκB from NF-κB that allows NF-κB translocation to the nucleus. NF-κB signaling plays a crucial role in the inflammatory cascade.

The purpose of this study was to determine if exposing human aortic valve interstitial cells (AVICs) to cyclic stretch activates inflammatory pathways and elucidate the mechanisms involved. Aortic valve calcification/stenosis (AVC) is the third leading cause of adult heart disease (6) and the most common form of acquired valvular disease in

Abbreviations: AVC, aortic valve calcification/stenosis; AVIC, aortic valve interstitial cell; BAV, bicuspid aortic valve; FDR, false discovery rate; IKKβ, IκB kinase β; miRNA, microRNA; miRNA-Seq, miRNA sequencing; MMP, metalloproteinase; NF-κB, nuclear factor kappa-light-chain-enhancer of activated B cells; PMA, phorbol-12-myristate-13-acetate; qPCR, quantitative PCR

[1] These authors contributed equally to this study.

[2] Correspondence: Department of Pediatrics (Cardiology), University of California San Diego, 9500 Gilman Drive Box 0731, La Jolla, CA 92093, USA. E-mail: vnigam@ucsd.edu

doi: 10.1096/fj.14-257808

This article includes supplemental data. Please visit *http://www.fasebj.org* to obtain this information.

developed countries (7). The risk factor most closely linked to calcific aortic stenosis is bicuspid aortic valve (BAV) (7–10) because 64% of calcified aortic valves have BAV morphology (11). BAVs experience increased stretch compared to normal tricuspid aortic valves every heartbeat (12, 13). Calcified aortic valves show markers of inflammation such as NF-$\kappa$B activation (14), ILs (15, 16), and metalloproteinases (MMPs) (15, 17–21), as well as an influx of inflammatory cells, primarily macrophages and T-lymphocytes (22–26).

Here we present evidence that human AVICs exposed to cyclic stretch have significantly increased expression of ILs and MMPs and secrete factors that activate monocytes/macrophages. Because miRNAs have been implicated in aortic valve disease (27–29), we performed miRNA sequencing (miRNA-Seq) to identify stretch responsive miRNAs. Among several differentially expressed miRNAs, we found that miR-148a-3p levels are decreased in stretched AVICs. By performing *in silico* analysis of our miRNA-Seq data, we identified *IKBKB,* a key activator of NF-$\kappa$B signaling, as a putative target of stretch repressed miR-148a-3p. Ectopic expression of miR-148a-3p in AVICs resulted in decreased *IKBKB* levels, NF-$\kappa$B signaling, and expression of NF-$\kappa$B target genes. On the basis of these results, we propose that stretch-induced repression of miR-148a-3p results in increased IKK$\beta$ levels, NF-$\kappa$B signaling, and up-regulation of NF-$\kappa$B target genes such as MMPs and ILs. These data support the hypothesis that AVICs exposed to increased biomechanical stressors can activate inflammatory pathways associated with AVC.

## MATERIAL AND METHODS

### Exposing human AVICs to cyclic stretch

Human aortic valve leaflets were collected from organ donors whose hearts could not be transplanted under an institutional review board exempt protocol and in accordance with the principles of the Declaration of Helsinki. Human AVICs were cultured according to standard protocols (30, 31). Cells, from passages 3 to 8, were grown on Collagen-1-coated Bioflex plates (BF-3001C; Flexcell International, Hillsborough, NC, USA). AVICs were exposed to cyclic stretch of 14% at 1 Hz using a Flexcell FX-5000 Tension system (Flexcell International) or static condition, the control condition, for 24 hours at the same time on Bioflex plates.

### RNA isolation

RNA was isolated using RNAeasy columns (74104; Qiagen, Venlo, The Netherlands) or Trizol (15596; Invitrogen, Carlsbad, CA, USA) according to the manufacturers' protocols.

### Microarray analysis

Using standard protocols, RNA was hybridized to Affymetrix Human Gene 1.0 gene chips. Three samples from each condition were studied. Data analysis was performed using the Genespring GX 11.5 software suite (Agilent, Santa Clara, CA, USA). The data were normalized using robust multiarray averaging and transformed around the median expression of the entire experiment. The static and stretch conditions were compared by a Student's $t$ test with a $P$ value of $\leq 0.05$ and Benjamini and Hochberg multiple testing correction. A total of 939 probes, representing 780 genes, were found to be significantly different between the 2 conditions.

### Quantitative PCR (qPCR) analysis

cDNA was prepared using Superscript III (Invitrogen). qRT-PCR was performed using TaqMan primers (Applied Biosystems, Foster City, CA, USA) and SYBR Green primers for a panel of calcification-related genes. To calculate relative expression levels, the $\Delta\Delta$Ct method was used, with normalization to glyceraldehyde phosphate dehydrogenase as the endogenous control.

### ELISA quantification

ELISA for IL-1$\beta$ and IL-8 were done in accordance with manufacturers' protocols (R&D Systems, Minneapolis, MN, USA).

### THP-1 differentiation

Undifferentiated THP-1 cells (American Type Culture Collection, Manassas, VA, USA) were plated in 24-well plates at $5 \times 10^5$ cell per well in unconditioned media (M199 + 10% fetal bovine serum) or conditioned media from AVICs. Conditioned media was collected from static AVICs or stretched AVICs. Cell adherence was used as a measure of differentiation of monocytes into macrophages (32). After 24 hours incubation, plates were washed 3 times with PBS to remove nonadherent cells. Adherent cells were lysed and quantified by total lactate dehydrogenase using the CytoTox 96 Non-Radioactive Cytotoxicity Assay kit (Promega, Madison, WI, USA) as per the manufacturer's protocol.

### THP-1 activation

THP-1 cells were treated with 50 ng/ml phorbol-12-myristate-13-acetate (PMA) to differentiate into adherent macrophages. The THP-1 cells were cultured in conditioned media from static or stretched AVICs for 24 hours before collecting for RNA analysis.

### Small RNA Library Preparation

Total RNA (1 $\mu$g) from 6 stretched and 6 static AVIC samples were used for small RNA library preparation using the TruSeq Small RNA protocol (Illumina, San Diego, CA, USA). All RNA was validated using an Agilent Bioanalyzer, and only samples with an RNA integrity number of >8 were used. Illumina adapters were ligated to each end of the RNA molecule, and a reverse transcriptase reaction was used to create single-stranded cDNA. The cDNA was subsequently PCR amplified using a universal primer and a primer containing 1 of 48 Illumina index sequences.

### miRNA deep sequencing

The small RNA libraries were loaded onto the Illumina cBot Cluster Station, where they bind to complementary adapter oligos grafted onto a proprietary flow cell substrate. Isothermal amplification of the cDNA construct was carried out creating clonal template clusters of approximately 1000 copies each. The Illumina HiSeq2500 directly sequences the resulting high-density array of template clusters on the flow cell using sequencing by

synthesis. Four proprietary fluorescently labeled, reversible terminator nucleotides were utilized to sequence the millions of clusters base by base in parallel.

For deep sequencing reads produced by the Illumina HiSeq2500, low-quality reads were filtered out to exclude those most likely to represent sequencing errors, and adaptor sequences were subsequently trimmed into clean full-length reads formatted into a nonredundant Fasta format. The occurrences of each unique sequence reads were counted as sequence tags (the number of reads for each tag reflects relative expression level); only small RNA sequences of 18 to 30 nt were retained for further analysis.

All unique sequence tags that passed above filters were mapped onto the reference human genome using the Bowtie2 program (33). The hits were counted using a custom Perl script, then translating the RNA IDs to gene IDs using the National Center for Biotechnology Information database (Bethesda, MD, USA). All counts that came from the same gene under that gene ID were added. The edgeR algorithm implemented under the Bioconductor suite was used to obtain expression levels and significance (*P* values, *q* values) (34).

### miRNA-qPCR

miRNA-qPCR was performed using standard techniques and TaqMan primers (Applied Biosystems). U6 was used as the endogenous control. Human diseased bicuspid valves were collected under a protocol approved by the institutional review board at the University Clinic of Schleswig-Holstein, Campus Luebeck, and in accordance with the principles of the Declaration of Helsinki (27). The control valves were obtained from organ donors whose hearts could not be used for transplantation under a University of California San Diego institutional review board–exempt protocol. RNA was isolated from the valve leaflets with Trizol.

### miRNA transfection

AVICs were transfected with either 100 pmol of miR-148a-3p mimic (Invitrogen) or scramble control using Lipofectamine 2000 (27) in 10 $cm^2$ wells. In the miRNA inhibitor experiments, AVICs were transfected with either 200 pmol of miR-148a-3p inhibitor or scramble control (Invitrogen). Cells were collected for RNA and protein analysis 72 hours after transfection.

### Western blot analysis

Western blot analysis was performed using $\alpha$-IKK$\beta$, $\alpha$-IKB$\alpha$, and $\alpha$-phospo-p65 (Cell Signaling Technology, Danvers, MA, USA) primary antibodies at 1:1000 dilution, horseradish peroxidase–conjugated $\alpha$-rabbit secondary antibody (GE Healthcare Life Sciences, Waukesha, WI, USA) was used at 1:10,000 dilution, and Western blots were developed by chemiluminescence. $\beta$-Actin was used as a loading control.

### Statistical analysis

The statistical significance of differences between groups was determined with the unpaired *t* test. $P \leq 0.05$ was considered significant. The SEM was calculated and is included in the graphs.

### HEK293 cell culture

HEK293 cells were maintained in DMEM (Life Technologies, Carlsbad, CA, USA) containing 10% heat-inactivated fetal bovine serum.

TABLE 1. *Ten most up-regulated genes*

| Gene symbol | Gene name | Fold change | Corrected *P*[a] |
|---|---|---|---|
| *IL-33* | Interleukin 33 | 8.27 | 0.011 |
| *MMP-1* | Matrix metallopeptidase 1 | 6.62 | 0.006 |
| *IL-1*β | Interleukin 1, $\beta$ | 5.71 | 0.005 |
| *TFPI-2* | Tissue factor pathway inhibitor 2 | 5.34 | 0.010 |
| *ANPEP* | Alanyl (membrane) aminopeptidase | 4.23 | 0.014 |
| *ANXA-10* | Annexin A10 | 4.17 | 0.010 |
| *AADAC* | Arylacetamide deacetylase (esterase) | 4.13 | 0.041 |
| *TOP-2*α | Topoisomerase (DNA) II$\alpha$ 170 kDa | 3.42 | 0.010 |
| *IL-13R*α*2* | Interleukin 13 receptor $\alpha$2 | 3.33 | 0.017 |
| *SHCBP-1* | SHC SH2-domain binding protein 1 | 3.11 | 0.022 |

[a]Genes had Benjamini and Hochberg multiple testing corrected *P* values of $<0.05$ ($n = 3$).

### Luciferase assays

The putative target sites from the 3′ UTR of the human *IKBKB* gene were cloned into the 3′ UTR of luciferase in the pMIRR-Luc reporter plasmid (Life Technologies). To create each clone, a pair of oligos (synthesized by Valuegene, San Diego, CA) was annealed, phosphorylated, and ligated into the *Spe*I and *Hin*dIII sites of pMIRR-Luc. For the 132–154 site reporter, the following oligos were used: 5′CTAGTTCACATGGTGGTTCCTGCTGCACTGATGGCCCAA-3′, 5′-AGCTTTGGGCCATCAGTGCAGCAGGAACCACCATGTGAA-3′. For the mutant 132–154 site reporter, the following oligos were used: 5′-CTAGTTCACATGGTGGTTCCTGCTGCTGAGATGGCCCAA-3′, 5′-AGCTTTGGGCCATCTCAGCAGCAGGAACCACCATGTGAA-3′. For the 1281–1303 site reporter, the following oligos were used: 5′-CTAGTCTTTGTGGAGATTCACACTATGCACTGGGAAAGA-3′, 5′-AGCTTCTTTCCCAGTGCATAGTGTGAATCTCCACAAAGA-3′.

For luciferase reporter assays, HEK293 cells were plated in 12-well plates, and each well was transfected with 2 $\mu$l Lipofectamine 2000 (Life Technologies), 75 ng of luciferase plasmid, and 30 ng of cytomegalovirus $\beta$-galactosidase vector (for normalization). With each plasmid, either scramble control or hsa-miR-148a-3p mimic (Life Technologies) was also transfected at a final concentration of 50 nM. Cells were collected and assayed 27 to 52 hours after transfection. Results represent 3 to 5 independent experiments for each plasmid. Luciferase assays and $\beta$-galactosidase assays were performed as previously described (35).

### Data sharing

The microarray data has been deposited at GEO as GSE47687. The miRNA-Seq raw data is available under GSE49558. The HeLa array data set is available at EBI under E-MTAB-2411.

TABLE 2. *IL family members modulated by stretch in our microarray data*

| Gene symbol | Gene name | Fold change | Corrected *P* value |
|---|---|---|---|
| *IL1*α | Interleukin 1, $\alpha$ | 2.51 | 0.022 |
| *IL1*β | Interleukin 1, $\beta$ | 5.71 | 0.005 |
| *IL8* | Interleukin 8 | 1.85 | 0.011 |
| *IL33* | Interleukin 33 | 8.27 | 0.011 |

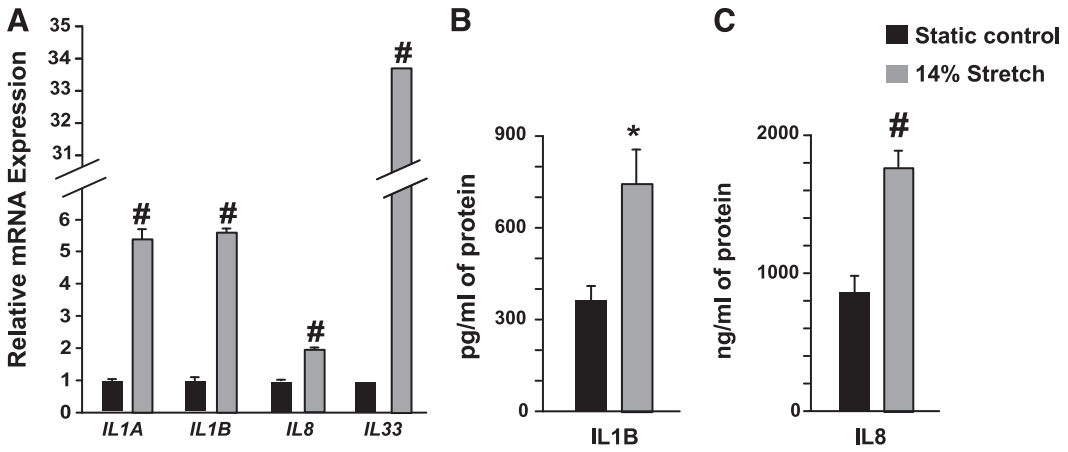


**Figure 1.** Cyclic stretch increases interleukin expression. *A*) qPCR showing increased mRNA levels for *IL-1*α, *IL-1*β, *IL-8,* and *IL-33*. *B, C*) ELISA demonstrating that stretched AVICs secrete increased amounts of IL-1$\beta$ and IL-8. *$P < 0.05$, #$P < 0.005$; $n = 3$.

## RESULTS

### Microarray profiling AVICs exposed to cyclic stretch demonstrates increased expression of inflammatory genes

Given that BAVs experience increased biomechanical strain, we examined the role that increased stretch plays in altering gene expression by exposing human AVICs to cyclic stretch *in vitro*. Cells were exposed to 14% stretch at 1 Hz, which corresponds to a physiologic heart rate of 60 beats per minute. The 14% stretch replicated the pathologic condition in BAVs; static condition was used as the control. Microarray analysis was performed on RNA from stretched and static control AVICs to identify stretch responsive genes in an unbiased manner. Analysis of the profiling data showed that 780 genes, 2.7% of the genes evaluated, were changed by >1.2-fold up or down with cyclic stretch using Benjamini and Hochberg multiple-testing-corrected *P* values of ≤0.05. Upon examination of the most up-regulated genes in AVICs by cyclic stretch (**Table 1**), we identified genes involved in inflammatory processes that are also found at higher levels in diseased aortic valves, such as *MMP-1* and *IL-1*β (15–21).

### Cyclic stretch increases expression of ILs and MMPs

Microarray profiling demonstrated that *IL*s and *MMP*s were among the most up-regulated genes in the stretched AVICs. Specifically, microarray data demonstrated that mRNA levels of *IL-1*α, *IL-1*β, *IL-8,* and *IL-33* were increased in a statistically significant manner >1.5-fold in stretched samples (**Table 2**). We performed qPCR to validate the changes in *IL* expression noted on the array (**Fig. 1*A***). ELISA assays showed that stretched AVICs have elevated levels of IL-1$\beta$ and IL-8 (Fig. 1*B, C*). Our microarray data suggested that several members of the MMP family (*MMP-1, MMP-14, MMP-16*) were up-regulated by cyclic stretch (**Table 3**). Expression changes of these MMPs were confirmed by qPCR (**Fig. 2**).

TABLE 3. *MMPs modulated by stretch in our microarray data set*

| Gene symbol | Gene name | Fold change | Corrected *P* value |
|---|---|---|---|
| *MMP1* | Matrix metallopeptidase 1 | 6.62 | 0.006 |
| *MMP10* | Matrix metallopeptidase 10 | 2.14 | 0.018 |
| *MMP14* | Matrix metallopeptidase 14 | 1.6 | 0.017 |
| *MMP16-1* | Matrix metallopeptidase 16 | 2.78 | 0.047 |
| *MMP16-2* | Matrix metallopeptidase 16 | 2.48 | 0.017 |

### Conditioned media from stretched AVICs activates monocytes/macrophages

Macrophages are frequently found in regions of AVC (22, 36). Inflammation genes, such as ILs, have been shown to activate macrophages. Thus, we examined whether the activation of the inflammatory genes by cyclic stretch can modulate activity of macrophages. Conditioned media from stretched AVIC cells was sufficient to induce differentiation of THP-1 monocytes into macrophages as determined by the THP-1 monocytes becoming adherent to

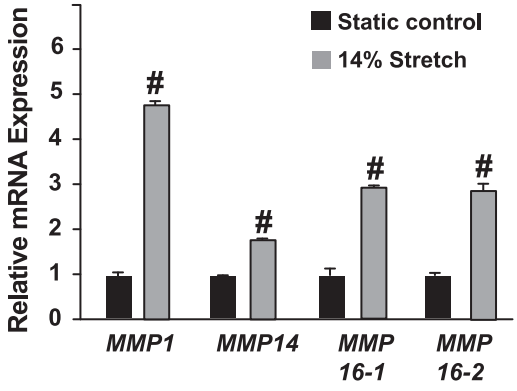


**Figure 2.** Cyclic stretch increased expression of MMPs. qPCR showing AVICs exposed to 14% cyclic stretch have increases in *MMP-1, MMP-14, MMP-16-1,* and *MMP-16-2* mRNA levels. #$P < 0.005$; $n = 3$.

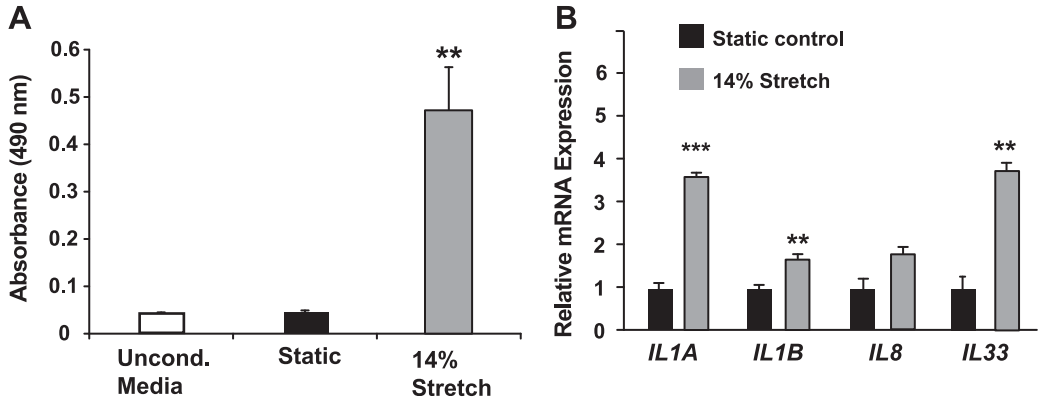


**Figure 3.** Conditioned media from stretched AVICs activates THP-1 macrophages. *A*) Differentiation of THP-1 monocytes into adherent macrophages, quantified by total lactate dehydrogenase assay performed on THP-1 cells treated with conditioned media from stretched or static AVICs for 24 h. *B*) THP-1 cells treated with conditioned media have increased expression of *IL-1*α, *IL-1*β, and *IL-33* compared to controls. $^{**}P < 0.01$, $\#P < 0.005$; $n = 3$.

tissue culture plates. Lactate dehydrogenase assays were used to quantitate the increased in cell adherence. We observed that conditioned media from static AVIC cells did not significantly induce more monocyte differentiation than unconditioned media, whereas a 10-fold increase ($P < 0.01$) in differentiation of monocytes was observed when THP-1 cells were grown in conditioned media from stretched AVICs (**Fig. 3A**). In addition, we studied the ability of conditioned media from static or stretched AVICs to activate THP-1 macrophages differentiated by PMA treatment. Differentiated THP-1 macrophages were cultured in conditioned media from AVICs exposed to static or cyclic stretch for 24 hours. THP-1 cells exposed to conditioned media from stretched cells showed increased activation, as demonstrated by an increase in expression of *IL-1*α, *IL-1*β, and *IL-33* (Fig. 3*B*).

### Identification of Stretch Responsive miRNAs by use of miRNA-Seq

Because miRNAs have been implicated in aortic valve disease (27–29), we performed miRNA-Seq to identify stretch responsive miRNAs in AVICs. We identified 15 miRNAs that were modulated by stretch with a false discovery rate (FDR) of <0.01 (**Table 4**).

NF-κB staining is increased in diseased aortic valves (14), and many of the stretch-activated ILs and MMPs are known NF-κB targets (37–41); therefore, we examined whether any of the stretch-mediated changes in miRNA levels would increase NF-κB signaling. We focused on miR-148a-3p because 7 different miRNA target algorithms (42–48) predict that miR-148a-3p targets *IKBKB*. miR-148a levels are decreased in stretched AVICs by 48% (FDR $1.42 \times 10^{-5}$) in our miRNA-Seq data (Table 2) and 43% ($P < 0.05$) by qPCR (**Fig. 4A**). miR-148a-3p was the 50th most abundant miRNA species in the miRNA-Seq data from AVICs in the static condition. Because BAV leaflets experience increased stretch, we compared miR-148a-3p levels from human BAV and tricuspid aortic valve leaflets to determine if miR-148a is modulated by stretch *in vivo*. We found that BAVs have 63% less miR-148a-3p ($P < 0.05$) compared to control aortic valve leaflets (Fig. 4*B*). Hence, we demonstrated that miR-148a is repressed by stretch both *in vitro* and *in vivo*.

### miR-148a represses NF-κB signaling

IKKβ, encoded by *IKBKB*, is a key regulator of NF-κB signaling because IKKβ inactivates IκB. *IKBKB* expression is increased by 47% in stretched AVICs in our microarray data ($P = 3.29 \times 10^{-4}$) and by 45% qPCR ($P < 0.05$) (Fig. 4*C*). To demonstrate that miR-148a-3p inhibits IKKβ and NF-κB signaling, we increased miR-148a-3p levels in AVIC by transfecting these cells with miR-148a-3p mimic. Cells treated with miR-148a mimic have decreased *IKBKB* mRNA and IKKβ protein levels compared to AVICs transfected with scramble control (Fig. 4*D, E*). AVICs with higher miR-148a-3p levels have decreased NF-κB signaling as demonstrated by increased IκB protein and decreased phospho-p65 protein levels (Fig. 4*E*).

To examine if miR-148a-3p directly targets the 3′ UTR of *IKBKB*, we performed luciferase assays to test whether the *in silico* data predicted 2 miR-148a-3p binding sites

TABLE 4. *Fifteen miRNAs that were stretch responsive with an FDR of <0.01*

| miRNA name | Fold change | FDR |
|---|---|---|
| hsa-miR-212 | 3.63 | 2.13E-13 |
| hsa-miR-132 | 1.72 | 3.58E-07 |
| hsa-miR-941 | 1.68 | 1.43E-09 |
| hsa-miR-486-5p | 1.59 | 2.99E-07 |
| hsa-miR-146a | 1.34 | 0.004 |
| hsa-miR-374a* | −1.34 | 0.009 |
| hsa-miR-143 | −1.34 | 0.004 |
| hsa-miR-148a-3p | −1.48 | 1.42E-05 |
| hsa-miR-335* | −1.67 | 3.13E-08 |
| hsa-miR-450b-5p | −1.67 | 0.0005 |
| hsa-miR-1197 | −1.73 | 0.0005 |
| hsa-miR-145 | −1.76 | 8.01E-09 |
| hsa-miR-19a | −1.83 | 4.33E-07 |
| hsa-miR-19b | −2.06 | 5.99E-15 |
| hsa-miR-1280 | −2.68 | 1.22E-21 |

*Part of the miRNA name.

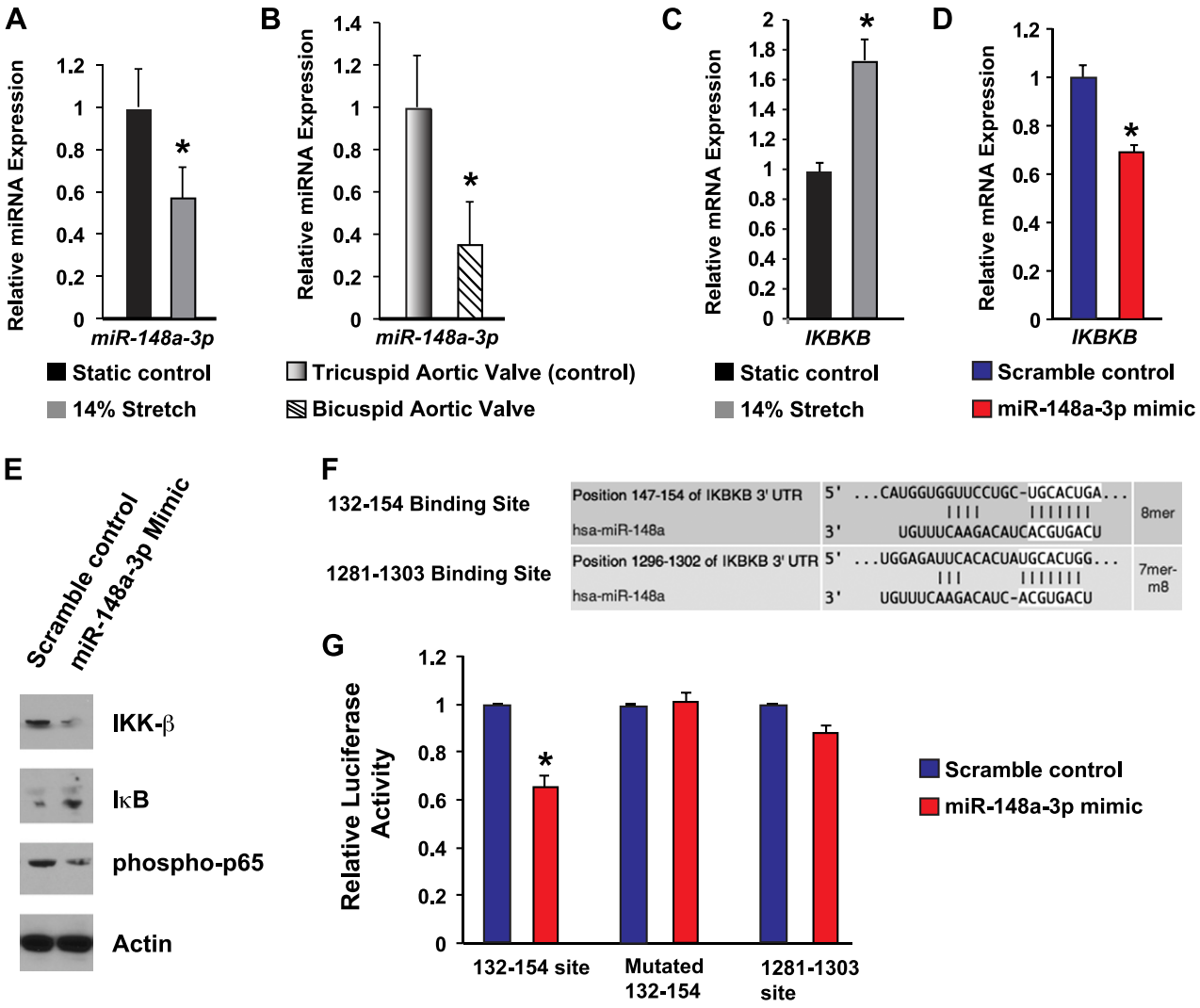


**Figure 4.** miR-148a-3p is repressed by stretch and represses both *IKBKB* and NF-κB signaling. *A*) qPCR demonstrates that AVICs exposed to cyclic stretch have decreased miR-148a-3p levels. *B*) Human diseased BAVs leaflets have decreased miR-148a-3p levels, determined by qPCR, compared to tricuspid aortic valves. *C*) *IKBKB* mRNA levels are increased in stretched AVICs compared to static controls. $^*P < 0.05$; $n = 4$. *D*) *IKBKB* mRNA levels were decreased by qPCR in miR-148a-3p mimic-treated AVICs compared to scramble controls. AVICs transfected with miR-148a-3p inhibitor did not have increased expression of *IKBKB*. *E*) Western blot analysis showing protein levels of IKK*β*, IκB, and phospho-p-65 after transfection with miR-148a-3p mimic. *F*) Targetscan miRNA target prediction algorithm predicts 2 miR-148a-3p binding sites in the 3′ UTR of *IKBKB*. *G*) Luciferase reporters bearing putative miR-148a binding sites were transfected into HEK293 cells. Reporter for the 132–154 site of the *IKBKB* 3′ UTR demonstrated a 35% reduction ($P < 0.02$) of luciferase when cotransfected with miR-148a-3p. The miR-148a-3p-mediated repression of this site was abrogated when 3 bases in the seed site was mutated. The 1281–1303 site was not significantly repressed by miR-148a-3p mimic, yielding a 12% reduction ($P = 0.06$); $n = 3$.

within the 3′ UTR of *IKBKB* (Fig. 4*F*) are modulated by miR-148a-3p. The luciferase activity of a construct containing the 132–154 binding site is decreased by miR-148a-3p cotransfection, demonstrating that this site is directly targeted by miR-148a-3p. The sequence specificity of the targeting of the 132–154 site is further confirmed by disruption of 3 bases within the seed binding site (bases 147–154), resulting in abrogation of miR-148a-3p repression. The 132–154 site is preferentially targeted because the luciferase activity of the 1281–1303 site construct was minimally reduced by miR-148a-3p. (Fig. 4*G*). Our findings demonstrate that miR-148a-3p is a novel repressor of *IKBKB* and NF-κB signaling.

### miR-148a-3p reduces expression of NF-κB target genes

Because members of the IL and MMP families are known NF-κB targets, we examined if miR-148a-3p represses expression of these ILs and MMPs. AVICs transfected with miR-148a-3p mimic have decreased expression of *IL-1α*, *IL-1β*, *IL-8*, *MMP-1*, *MMP-14*, and *MMP-16* (**Fig. 5*A, B***). miR-148a-3p is sufficient to block/attenuate the stretch activation of *IKBKB*, *IL-1*β, *IL-8*, *MMP-1*, and *MMP-14* (Fig. 5*C*). Treatment with miR-148a-3p inhibitor resulted in increased expression of *IL-1*α, *IL-1*β, *IL-8*, *IL-33*, *MMP-1*, and *MMP-16* (Fig. 5*D, E*), thereby providing further evidence that miR-148a represses the expression of key inflammatory genes. In

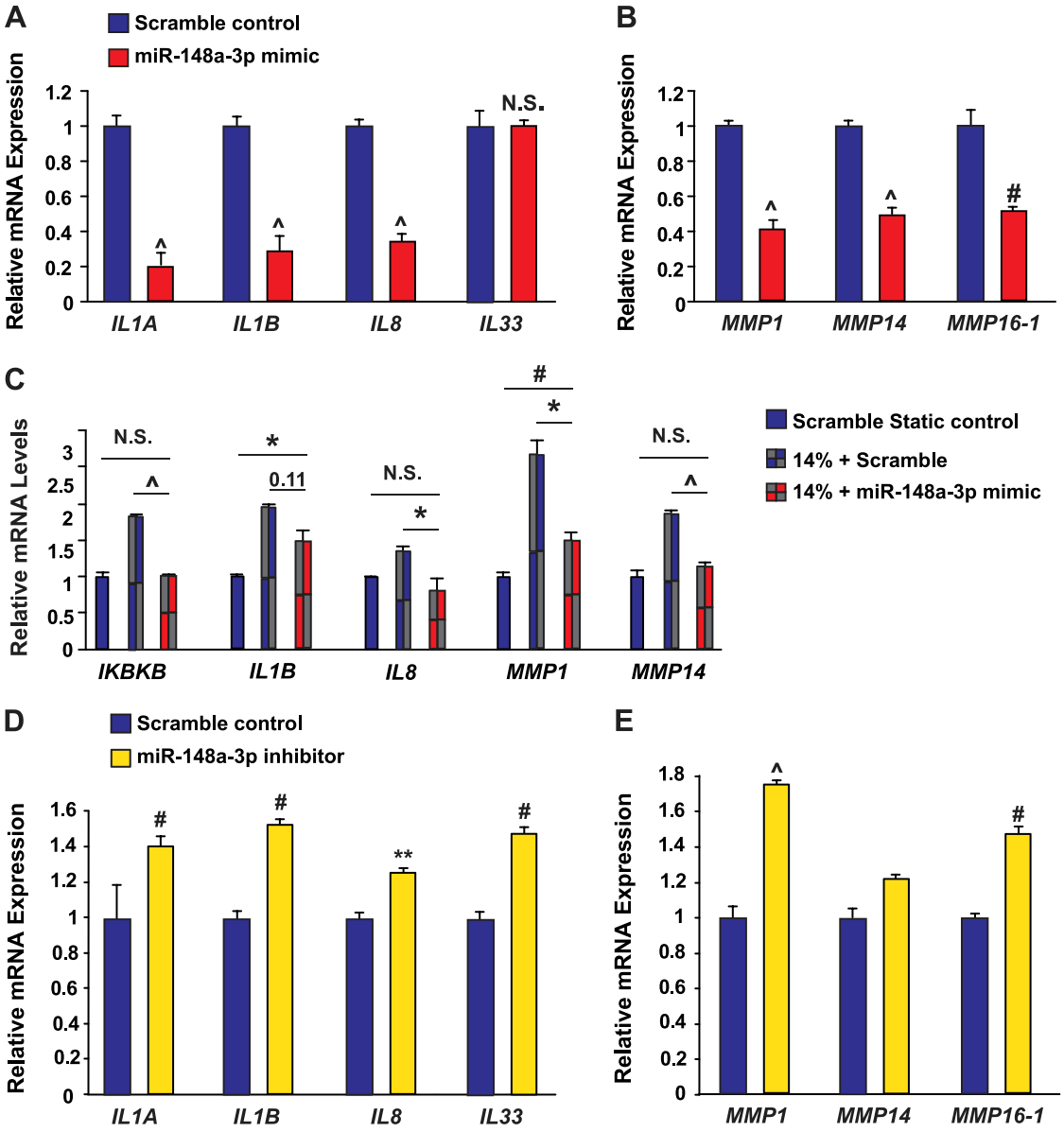


**Figure 5.** miR-148a represses expression of inflammatory genes. AVICs were transfected with miR-148a mimic for 72 hours. *A*) The expression levels of ILs after transfection with miR-148a-3p mimic; $n = 6$. *B*) Expression of *MMP*s after transfection with miR-148a-3p mimic; $n = 6$. *C*) miR-148a mimic blocks/attenuates the stretch activation of *IKBKB, IL*-1β, *IL-8, MMP-1,* and *MMP-14.* AVICs were transfected with the scramble control or miR-148a-3p mimic 24 hours before being exposed to stretch or static conditions for 24 hours; $n = 3$. *D*) Transfection with miR-148a-3p inhibitor results in increased expression of ILs; $n = 4$. *E*) miR-148a inhibition results in increased expression of *MMP-1* and *MMP-16-1.* Of note, the expression levels of *MMP-14* trended toward being increased by miR-148a-3p inhibition ($P = 0.06$); $n = 4$. $*P < 0.05$, $\#P < 0.005$, $\wedge P < 0.001$.

addition, the analysis of gene expression changes in HeLa cells transfected with miR-148a-3p mimic demonstrate that miR-148a-3p modulates genes and gene ontology groups associated with inflammatory response ($P = 8.1 \times 10^{-6}$) and immune response ($4.59 \times 10^{-34}$) (Supplemental Data). These data demonstrate that miR-148a-3p is sufficient to inhibit expression of NF-κB target genes.

## DISCUSSION

In this report, we demonstrate that AVICs exposed to cyclic stretch have increased expression of inflammatory genes associated with AVC. Furthermore, the stretched AVICs secrete factors that can activate monocytes/macrophages because conditioned media from stretched AVICs increase adherence and activation of THP-1 cells. Our experimental and bioinfomatic data suggest that stretch repression of miR-148a-3p results in increased expression of inflammatory genes. In contrast to the majority of previous work in AVC, which is focused on genetic and atherosclerosis etiologies, our data provide evidence that the increased strain experienced by AVICs in BAVs is sufficient to activate the inflammatory pathways associated with AVC in a tissue-autonomous manner.

Although it has been shown that calcified aortic valves demonstrate inflammatory changes, to our knowledge,

our study is the first to report that exposing AVICs to stretch, similar to that experienced by BAVs, is sufficient to activate IL family member gene expression and monocytes/macrophages. MMP-1, MMP-2, and/or MMP-9 levels are increased in porcine aortic valve leaflets exposed to stretch (49). Our findings indicate that additional members of the MMP family, MMP-14/16, were increased in human AVICs exposed to cyclic stretch. MMP-14/16 are pro-MMP-2 (50); they are required for the activation of MMP-2, which in turns activates MMP-9. Thus, the increased biomechanical stretch imposed on AVICs in BAVs can activate expression of inflammatory genes.

Others have reported that porcine AVICs exposed to cyclic stretch have decreased expression of inflammatory genes (51). That study was based on qPCR for 4 genes that were decreased in stretched porcine AVICs: *Vcam-1, Mcp-1,* and *Gm-Csf* compared to static controls. Our conclusions were based upon a more comprehensive and unbiased microarray analysis, confirmed by RT-PCR and ELISA, and functional studies showing activation of monocytes/macrophages using human cells. Therefore, we have concluded that increased stretch of AVICs is sufficient to activate inflammatory pathways in human AVICs in a cell autonomous manner.

For our *in vitro* studies, we have exposed AVICs to isotropic cyclic stretch 14%. Although human tricuspid aortic valves have a well-organized aortic valve cell orientation, it has been recently reported that human BAVs have disorganized organization (52). Given this disorganization, isotropic strain is a starting point to examine the stretch responsive molecular pathways in BAV AVICs. Anisotropic strains are an interesting topic to study because we have found that BAVs experience anisotropic strains in *ex vivo* experiments (13). In addition, there are interesting data that porcine AVICs have differential responses to anisotropic strain (53). Although we have found BAV leaflets can experience as high as 25% increase in strain (13), a 14% strain for our experiments was used because that was the maximum strain that the Flexcell system could deliver at 1 Hz. Exposing human AVICs to anisotropic strains and different magnitudes of strain has potential to further the understanding of the role that stretch plays in the pathogenesis of BAV calcification.

We have found that miR-148a-3p is decreased both in stretched AVICs and diseased human BAV leaflets. Furthermore, miR-148a-3p targets *IKBKB,* thereby repressing NF-$\kappa$B signaling. We have shown that miR-148a-3p targets a site within the 3′ UTR of *IKBKB*. It is interesting to note that we identified a different set of stretch responsive miRNAs than the only previous report profiling stretch responsive miRNAs (54). This difference is most likely due to the difference between the different cell types examined. Alternatively, it could be due to different profiling modalities that were used. Although 3 other miRNAs have been reported to target *IKBKB* (3–5), this is the first report to indicate that miR-148a-3p targets *IKBKB,* thereby repressing NF-$\kappa$B signaling. The levels of these 3 other miRNAs—mir-199a, -200c, and -218—were not changed in our miRNA-Seq data set. We have demonstrated that stretch represses miR-148a levels both *in vitro* and *in vivo* and that miR-148a-3p is a novel repressor of NF-$\kappa$B signaling.

Our data demonstrate that miR-148a-3p is sufficient and necessary to repress the expression of IL and MMP family members that are known to be NF-$\kappa$B target genes. In addition, we have found that miR-148a-3p modulates inflammatory genes in microarray analyses (Supplemental Data). Our data demonstrate that miR-148a-3p mimic is sufficient to block or reduce the stretch activation of several inflammatory genes (Fig. 5*C*). There are several pieces of data that suggest that stretch modulation of miR-148a-3p is not the sole mechanism by which stretch activates inflammatory pathways. For example, miR-148a-3p mimic does not block the stretch-mediated increased expression of *IL-1*$\alpha$ and *MMP-16*. Additionally, conditioned media from AVICs transfected with miR-148a-3p inhibitor was not sufficient to activate THP-1 cells. Potential stretch responsive pathways may include stretch activation of miRNAs such as miR-132, miR-212, and miR-486-3p because these miRNAs may play roles in activating inflammatory pathways (55, 56). Given our data that miR-148a-3p can repress inflammatory genes and that other miRNAs are in

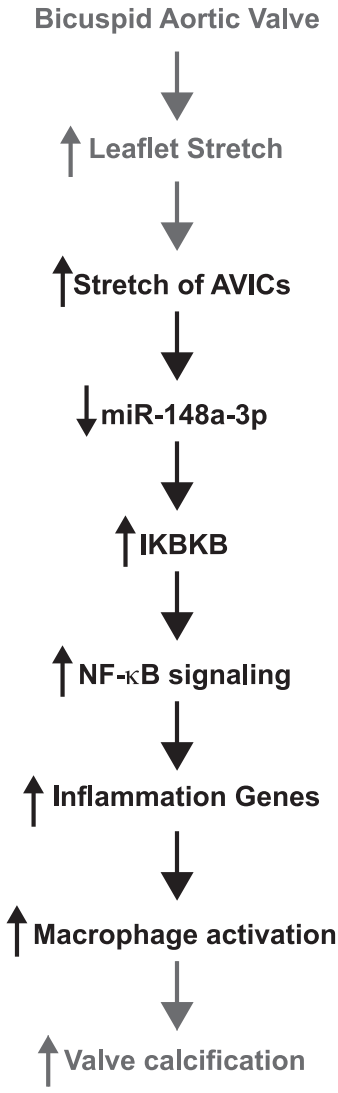


**Figure 6.** Model of how stretch activates NF-$\kappa$B signaling and inflammatory pathways. Black summarizes stretch responsive pathway based on our data. Gray indicates data in context of proposed mechanism by which BAVs develop AVC as the result of mechanical stretch due to their abnormal valve morphology.

clinical trials (57), miR-148a-3p-based treatments have potential as therapeutic modalities for AVC and other diseases that involve increased NF-κB signaling such as autoimmune diseases and cancer.

In conclusion, we have presented evidence that exposing human AVICs to cyclic stretch is sufficient to activate inflammatory pathways in a tissue-autonomous manner. As outlined in **Fig. 6**, the stretch-mediated activation involves repression of miR-148a-3p that allows for increased NF-κB signaling and inflammatory gene expression. Our findings suggest increasing miR-148a-3p levels in the aortic valve could be developed into treatment for AVC in individuals with BAVs. More broadly, the data presented here may for the first time help elucidate a mechanism by which a stretch responsive microRNA modulates NF-κB. FJ

The authors would like to thank Lifesharing for their assistance in obtaining the human valve tissue. The authors also thank Drs. I. Banerjee and S. Lange for technical assistance. They also acknowledge the University of California, San Diego (UCSD) Microarray and Biomedical Genomics Microarray Core Facilities for their assistance with the miRNA-Seq and microarray experiments. A.H. was funded by a CJ Martin—Biomedical Overseas fellowship from the Australian National Health and Medical Research Council. A.H. was funded by the Larry L. Hillblom Foundation. V.N. was supported by U.S. National Institutes of Health, National Heart, Lung, and Blood Institute Grant K08 HL086775-01 and the UCSD Department of Pediatrics.

## REFERENCES

1. Du, W., Mills, I., and Sumpio, B. E. (1995) Cyclic strain causes heterogeneous induction of transcription factors, AP-1, CRE binding protein and NF-kB, in endothelial cells: species and vascular bed diversity. *J. Biomech.* **28**, 1485–1491
2. Hishikawa, K., Oemar, B. S., Yang, Z., and Lüscher, T. F. (1997) Pulsatile stretch stimulates superoxide production and activates nuclear factor-kappa B in human coronary smooth muscle. *Circ. Res.* **81**, 797–803
3. Panda, H., Pelakh, L., Chuang, T. D., Luo, X., Bukulmez, O., and Chegini, N. (2012) Endometrial miR-200c is altered during transformation into cancerous states and targets the expression of ZEBs, VEGFA, FLT1, IKKβ, KLF9, and FBLN5. *Reprod. Sci.* **19**, 786–796
4. Chen, R., Alvero, A. B., Silasi, D. A., Kelly, M. G., Fest, S., Visintin, I., Leiser, A., Schwartz, P. E., Rutherford, T., and Mor, G. (2008) Regulation of IKKbeta by miR-199a affects NF-kappaB activity in ovarian cancer cells. *Oncogene* **27**, 4712–4723
5. Song, L., Huang, Q., Chen, K., Liu, L., Lin, C., Dai, T., Yu, C., Wu, Z., and Li, J. (2010) miR-218 inhibits the invasive ability of glioma cells by direct downregulation of IKK-β. *Biochem. Biophys. Res. Commun.* **402**, 135–140
6. American Heart Association. (2004) *Heart Disease and Stroke Statistics—2004 Update.* American Heart Association, Dallas
7. Freeman, R. V., and Otto, C. M. (2005) Spectrum of calcific aortic valve disease: pathogenesis, disease progression, and treatment strategies. *Circulation* **111**, 3316–3326
8. Ward, C. (2000) Clinical significance of the bicuspid aortic valve. *Heart* **83**, 81–85
9. Fedak, P. W., Verma, S., David, T. E., Leask, R. L., Weisel, R. D., and Butany, J. (2002) Clinical and pathophysiological implications of a bicuspid aortic valve. *Circulation* **106**, 900–904
10. Beppu, S., Suzuki, S., Matsuda, H., Ohmori, F., Nagata, S., and Miyatake, K. (1993) Rapidity of progression of aortic stenosis in patients with congenital bicuspid aortic valves. *Am. J. Cardiol.* **71**, 322–327
11. Davies, M. J., Treasure, T., and Parker, D. J. (1996) Demographic characteristics of patients undergoing aortic valve replacement for stenosis: relation to valve morphology. *Heart* **75**, 174–178
12. Robicsek, F., Thubrikar, M. J., Cook, J. W., and Fowler, B. (2004) The congenitally bicuspid aortic valve: how does it function? Why does it fail? *Ann. Thorac. Surg.* **77**, 177–185
13. Szeto, K., Pastuszko, P., del Álamo, J. C., Lasheras, J., and Nigam, V. (2013) Bicuspid aortic valves experience increased strain as compared to tricuspid aortic valves. *World J. Pediatr. Congenit. Heart Surg.* **4**, 362–366
14. Steinmetz, M., Skowasch, D., Wernert, N., Welsch, U., Preusse, C. J., Welz, A., Nickenig, G., and Bauriedel, G. (2008) Differential profile of the OPG/RANKL/RANK-system in degenerative aortic native and bioprosthetic valves. *J. Heart Valve Dis.* **17**, 187–193
15. Kaden, J. J., Dempfle, C. E., Grobholz, R., Tran, H. T., Kiliç, R., Sarikoç, A., Brueckmann, M., Vahl, C., Hagl, S., Haase, K. K., and Borggrefe, M. (2003) Interleukin-1 beta promotes matrix metalloproteinase expression and cell proliferation in calcific aortic valve stenosis. *Atherosclerosis* **170**, 205–211
16. Naito, Y., Tsujino, T., Wakabayashi, K., Matsumoto, M., Ohyanagi, M., Mitsuno, M., Miyamoto, Y., Hao, H., Hirota, S., Okamura, H., and Masuyama, T. (2010) Increased interleukin-18 expression in nonrheumatic aortic valve stenosis. *Int. J. Cardiol.* **144**, 260–263
17. Kaden, J. J., Dempfle, C. E., Grobholz, R., Fischer, C. S., Vocke, D. C., Kiliç, R., Sarikoç, A., Piñol, R., Hagl, S., Lang, S., Brueckmann, M., and Borggrefe, M. (2005) Inflammatory regulation of extracellular matrix remodeling in calcific aortic valve stenosis. *Cardiovasc. Pathol.* **14**, 80–87
18. Edep, M. E., Shirani, J., Wolf, P., and Brown, D. L. (2000) Matrix metalloproteinase expression in nonrheumatic aortic stenosis. *Cardiovasc. Pathol.* **9**, 281–286
19. Soini, Y., Satta, J., Määttä, M., and Autio-Harmainen, H. (2001) Expression of MMP2, MMP9, MT1-MMP, TIMP1, and TIMP2 mRNA in valvular lesions of the heart. *J. Pathol.* **194**, 225–231
20. Satta, J., Oiva, J., Salo, T., Eriksen, H., Ohtonen, P., Biancari, F., Juvonen, T. S., and Soini, Y. (2003) Evidence for an altered balance between matrix metalloproteinase-9 and its inhibitors in calcific aortic stenosis. *Ann. Thorac. Surg.* **76**, 681–688, discussion 688
21. Fondard, O., Detaint, D., Iung, B., Choqueux, C., Adle-Biassette, H., Jarraya, M., Hvass, U., Couetil, J. P., Henin, D., Michel, J. B., Vahanian, A., and Jacob, M. P. (2005) Extracellular matrix remodelling in human aortic valve disease: the role of matrix metalloproteinases and their tissue inhibitors. *Eur. Heart J.* **26**, 1333–1341
22. Otto, C. M., Kuusisto, J., Reichenbach, D. D., Gown, A. M., and O'Brien, K. D. (1994) Characterization of the early lesion of "degenerative" valvular aortic stenosis. Histological and immunohistochemical studies. *Circulation* **90**, 844–853
23. Olsson, M., Dalsgaard, C. J., Haegerstrand, A., Rosenqvist, M., Rydén, L., and Nilsson, J. (1994) Accumulation of T lymphocytes and expression of interleukin-2 receptors in nonrheumatic stenotic aortic valves. *J. Am. Coll. Cardiol.* **23**, 1162–1170
24. Wallby, L., Janerot-Sjöberg, B., Steffensen, T., and Broqvist, M. (2002) T lymphocyte infiltration in non-rheumatic aortic stenosis: a comparative descriptive study between tricuspid and bicuspid aortic valves. *Heart* **88**, 348–351
25. Mohler III, E. R., Adam, L. P., McClelland, P., Graham, L., and Hathaway, D. R. (1997) Detection of osteopontin in calcified human aortic valves. *Arterioscler. Thromb. Vasc. Biol.* **17**, 547–552
26. O'Brien, K. D., Kuusisto, J., Reichenbach, D. D., Ferguson, M., Giachelli, C., Alpers, C. E., and Otto, C. M. (1995) Osteopontin is expressed in human aortic valvular lesions. *Circulation* **92**, 2163–2168
27. Nigam, V., Sievers, H. H., Jensen, B. C., Sier, H. A., Simpson, P. C., Srivastava, D., and Mohamed, S. A. (2010) Altered microRNAs in bicuspid aortic valve: a comparison between stenotic and insufficient valves. *J. Heart Valve Dis.* **19**, 459–465
28. Yanagawa, B., Lovren, F., Pan, Y., Garg, V., Quan, A., Tang, G., Singh, K. K., Shukla, P. C., Kalra, N. P., Peterson, M. D., and Verma, S. (2012) miRNA-141 is a novel regulator of BMP-2-mediated calcification in aortic stenosis. *J. Thorac. Cardiovasc. Surg.* **144**, 256–262
29. Holliday, C. J., Ankeny, R. F., Jo, H., and Nerem, R. M. (2011) Discovery of shear- and side-specific mRNAs and miRNAs in human aortic valvular endothelial cells. *Am. J. Physiol. Heart Circ. Physiol.* **301**, H856–H867

30. Jian, B., Narula, N., Li, Q. Y., Mohler, E. R., 3rd, and Levy, R. J. (2003) Progression of aortic valve stenosis: TGF-beta1 is present in calcified aortic valve cusps and promotes aortic valve interstitial cell calcification via apoptosis. *Ann. Thorac Surg.* **75**, 457–465
31. Osman, L., Yacoub, M. H., Latif, N., Amrani, M., and Chester, A. H. (2006) Role of human valve interstitial cells in valve calcification and their response to atorvastatin. *Circulation* **114**(1, Suppl)I547–I552
32. Park, E. K., Jung, H. S., Yang, H. I., Yoo, M. C., Kim, C., and Kim, K. S. (2007) Optimized THP-1 differentiation is required for the detection of responses to weak stimuli. *Inflamm. Res.* **56**, 45–50
33. Langmead, B., Trapnell, C., Pop, M., and Salzberg, S. L. (2009) Ultrafast and memory-efficient alignment of short DNA sequences to the human genome. *Genome Biol.* **10**, R25
34. Robinson, M. D., McCarthy, D. J., and Smyth, G. K. (2010) edgeR: a Bioconductor package for differential expression analysis of digital gene expression data. *Bioinformatics* **26**, 139–140
35. Brasier, A. R., Tate, J. E., and Habener, J. F. (1989) Optimized use of the firefly luciferase assay as a reporter gene in mammalian cell lines. *Biotechniques* **7**, 1116–1122
36. Tanaka, K., Sata, M., Fukuda, D., Suematsu, Y., Motomura, N., Takamoto, S., Hirata, Y., and Nagai, R. (2005) Age-associated aortic stenosis in apolipoprotein E–deficient mice. *J. Am. Coll. Cardiol.* **46**, 134–141
37. Meng, X., Ao, L., Song, Y., Babu, A., Yang, X., Wang, M., Weyant, M. J., Dinarello, C. A., Cleveland, J. C., Jr., and Fullerton, D. A. (2008) Expression of functional Toll-like receptors 2 and 4 in human aortic valve interstitial cells: potential roles in aortic valve inflammation and stenosis. *Am. J. Physiol. Cell Physiol.* **294**, C29–C35
38. Mori, N., and Prager, D. (1996) Transactivation of the interleukin-1alpha promoter by human T-cell leukemia virus type I and type II Tax proteins. *Blood* **87**, 3410–3417
39. Hiscott, J., Marois, J., Garoufalis, J., D'Addario, M., Roulston, A., Kwan, I., Pepin, N., Lacoste, J., Nguyen, H., Bensi, G., et al. (1993) Characterization of a functional NF-kappa B site in the human interleukin 1 beta promoter: evidence for a positive autoregulatory loop. *Mol. Cell. Biol.* **13**, 6231–6240
40. Kang, H. B., Kim, Y. E., Kwon, H. J., Sok, D. E., and Lee, Y. (2007) Enhancement of NF-kappaB expression and activity upon differentiation of human embryonic stem cell line SNUhES3. *Stem Cells Dev.* **16**, 615–623
41. Vincenti, M. P., Coon, C. I., and Brinckerhoff, C. E. (1998) Nuclear factor kappaB/p50 activates an element in the distal matrix metalloproteinase 1 promoter in interleukin-1beta-stimulated synovial fibroblasts. *Arthritis Rheum.* **41**, 1987–1994
42. Dweep, H., Sticht, C., Pandey, P., and Gretz, N. (2011) miRWalk—database: prediction of possible miRNA binding sites by "walking" the genes of three genomes. *J. Biomed. Inform.* **44**, 839–847
43. Maragkakis, M., Reczko, M., Simossis, V. A., Alexiou, P., Papadopoulos, G. L., Dalamagas, T., Giannopoulos, G., Goumas, G., Koukis, E., Kourtis, K., Vergoulis, T., Koziris, N., Sellis, T., Tsanakas, P., and Hatzigeorgiou, A. G. (2009) DIANA-microT web server: elucidating microRNA functions through target prediction. *Nucleic Acids Res.* **37**, W273–W276
44. John, B., Enright, A. J., Aravin, A., Tuschl, T., Sander, C., and Marks, D. S. (2004) Human MicroRNA targets. *PLoS Biol.* **2**, e363
45. Wang, X. (2008) miRDB: a microRNA target prediction and functional annotation database with a wiki interface. *RNA* **14**, 1012–1017
46. Krek, A., Grün, D., Poy, M. N., Wolf, R., Rosenberg, L., Epstein, E. J., MacMenamin, P., da Piedade, I., Gunsalus, K. C., Stoffel, M., and Rajewsky, N. (2005) Combinatorial microRNA target predictions. *Nat. Genet.* **37**, 495–500
47. Kertesz, M., Iovino, N., Unnerstall, U., Gaul, U., and Segal, E. (2007) The role of site accessibility in microRNA target recognition. *Nat. Genet.* **39**, 1278–1284
48. Lewis, B. P., Burge, C. B., and Bartel, D. P. (2005) Conserved seed pairing, often flanked by adenosines, indicates that thousands of human genes are microRNA targets. *Cell* **120**, 15–20
49. Balachandran, K., Sucosky, P., Jo, H., and Yoganathan, A. P. (2009) Elevated cyclic stretch alters matrix remodeling in aortic valve cusps: implications for degenerative aortic valve disease. *Am. J. Physiol. Heart Circ. Physiol.* **296**, H756–H764
50. Zhao, H., Bernardo, M. M., Osenkowski, P., Sohail, A., Pei, D., Nagase, H., Kashiwagi, M., Soloway, P. D., DeClerck, Y. A., and Fridman, R. (2004) Differential inhibition of membrane type 3 (MT3)-matrix metalloproteinase (MMP) and MT1-MMP by tissue inhibitor of metalloproteinase (TIMP)-2 and TIMP-3 rgulates pro-MMP-2 activation. *J. Biol. Chem.* **279**, 8592–8601
51. Smith, K. E., Metzler, S. A., and Warnock, J. N. (2010) Cyclic strain inhibits acute pro-inflammatory gene expression in aortic valve interstitial cells. *Biomech. Model. Mechanobiol.* **9**, 117–125
52. Aggarwal, A., Ferrari, G., Joyce, E., Daniels, M. J., Sainger, R., Gorman III, J. H., Gorman, R., and Sacks, M. S. (2014) Architectural trends in the human normal and bicuspid aortic valve leaflet and its relevance to valve disease. *Ann. Biomed. Eng.* **42**, 986–998
53. Gould, R. A., Chin, K., Santisakultarm, T. P., Dropkin, A., Richards, J. M., Schaffer, C. B., and Butcher, J. T. (2012) Cyclic strain anisotropy regulates valvular interstitial cell phenotype and tissue remodeling in three-dimensional culture. *Acta Biomater.* **8**, 1710–1719
54. Mohamed, J. S., Lopez, M. A., and Boriek, A. M. (2010) Mechanical stretch up-regulates microRNA-26a and induces human airway smooth muscle hypertrophy by suppressing glycogen synthase kinase-3β. *J. Biol. Chem.* **285**, 29336–29347
55. Strum, J. C., Johnson, J. H., Ward, J., Xie, H., Feild, J., Hester, A., Alford, A., and Waters, K. M. (2009) MicroRNA 132 regulates nutritional stress–induced chemokine production through repression of SirT1. *Mol. Endocrinol.* **23**, 1876–1884
56. Song, L., Lin, C., Gong, H., Wang, C., Liu, L., Wu, J., Tao, S., Hu, B., Cheng, S. Y., Li, M., and Li, J. (2013) miR-486 sustains NF-κB activity by disrupting multiple NF-κB-negative feedback loops. *Cell Res.* **23**, 274–289
57. Janssen, H. L., Reesink, H. W., Lawitz, E. J., Zeuzem, S., Rodriguez-Torres, M., Patel, K., van der Meer, A. J., Patick, A. K., Chen, A., Zhou, Y., Persson, R., King, B. D., Kauppinen, S., Levin, A. A., and Hodges, M. R. (2013) Treatment of HCV infection by targeting microRNA. *N. Engl. J. Med.* **368**, 1685–1694

*Received for publication June 16, 2014.*
*Accepted for publication December 22, 2014.*